

Symmetry energy dependence of the pygmy and giant dipole resonances in an isospin dependent quantum molecular dynamics model

TAO Cheng^{1,2} MA Yugang^{1,*} ZHANG Guoqiang¹ CAO Xiguang¹
FANG Deqing¹ WANG Hongwei¹

¹Shanghai Institute of Applied Physics, Chinese Academy of Sciences, Jiading Campus, Shanghai 201800, China

²University of Chinese Academy of Sciences, Beijing 100049, China

Abstract Isospin-dependent Quantum Molecular Dynamics model (IQMD) has been applied to investigate the Pygmy Dipole Resonance (PDR) and Giant Dipole Resonance (GDR) in Ni isotopes by Coulomb excitation. By Gaussian fitting to the photon emission spectra, the peak energies and strengths of PDR and GDR are extracted. Their sensitivities to impact parameter, incident energy and the symmetry energy are discussed. By the comparison of energy-weighted sum rule (EWSR) with the data and other calculations for ⁶⁸Ni, the parameters of density-dependence of symmetry energy in the IQMD are constrained. In addition, the N/Z dependence of PDR and GDR parameters of Ni isotopes are investigated, and the results that the EWSR increases linearly with the N/Z are obtained.

Key words Pygmy dipole resonance, Giant dipole resonance, Energy-weighted sum rule, Symmetry energy

1 Introduction

In the past decades, many works have been done on Pygmy Dipole Resonance (PDR) and Giant Dipole Resonance (GDR) both theoretically and experimentally^[1-4]. PDR or GDR is classic collective mode of nuclei, which can be considered as the vibration of valence neutrons against the nuclear core or neutrons against protons, respectively.

The results of many works show that the PDR plays an important role in neutron-capture rates in the r-process, nucleosynthesis, the radiative neutron-capture cross section on neutron-rich nuclei, as well as the photodisintegration of ultra-high energy cosmic rays^[5-18]. Recently, the correlation between PDR and symmetry energy has also been studied^[12,19].

In the present work, we try to apply the Isospin-dependent Quantum Molecular Dynamics (IQMD) model to investigate PDR and GDR in Ni isotopes.

2 Model and methods

In this section, we introduce the model and formulae which we used in the present calculation as well as the method how we choose the valence neutrons.

2.1 Isospin-dependent quantum molecular dynamical model

The Isospin-dependent Quantum Molecular Dynamics model which is based on QMD model is a kind of Monte-Carlo transport model^[20-25]. It has been extensively applied in heavy-ion collision dynamics.

In our IQMD model, the mean field can be written as follows:

$$U(\rho) = U^{\text{Sky}} + U^{\text{Coul}} + U^{\text{Yuk}} + U^{\text{sym}} + U^{\text{MDI}} \quad (1)$$

Here, U^{Sky} , U^{Coul} , U^{Yuk} , U^{sym} and U^{MDI} is the Skyrme potential, Coulomb potential, Yukawa potential, symmetry potential and Momentum Dependent Interaction (MDI), respectively.

Supported by the National Natural Science Foundation of China (Nos.11220101005, 11035009, 10979074 and 11205230) and Major State Basic Research Development Program in China (No.2013CB834405)

* Corresponding author. E-mail address: ygma@sinap.ac.cn

Received date: 2013-03-27

The Skyrme potential is given as follows:

$$U^{\text{Sky}} = \alpha(\rho/\rho_0) + \beta(\rho/\rho_0)^\sigma \quad (2)$$

Where ρ_0 is the saturation nuclear density ($\rho_0=0.16/\text{fm}^3$) and ρ is the nuclear density. Parameters $[\alpha, \beta, \sigma]$ which

Table 1 Parameters $[\alpha, \beta, \sigma]$ for different EOS

EOS	K / MeV	α / MeV	β / MeV	σ / MeV
S	200	-356	303	7/6
SM	200	-390.1	320.3	1.14
H	380	-124	70.5	2
HM	380	-129.2	59.4	2.09

The Coulomb potential can be written as follows:

$$U^{\text{Coul}} = \frac{e^2}{4} \sum_{i \neq j} \frac{1}{(4\pi L)^{3/2}} \exp\left[-\frac{|r_i - r_j|^2}{4L}\right] \quad (3)$$

where $r_{ij} = |r_i - r_j|$ represents the relative distance of two nucleons. And L is the so-called Gaussian wave-packet width for nucleons which a constant $L=2.16 \text{ fm}^2$ is used here.

The Yukawa potential can be written as follows:

$$U^{\text{Yuk}} = (V_y/2) \sum_{i \neq j} \frac{1}{r_{ij}} \exp(Lm^2) \times [\exp(mr_{ij}) \text{erfc}(\sqrt{L}m - r_{ij}/\sqrt{4L}) - \exp(mr_{ij}) \text{erfc}(\sqrt{L}m + r_{ij}/\sqrt{4L})] \quad (4)$$

where $V_y=0.0024 \text{ GeV}$, $m = 0.83$.

The symmetry potential can be written as follows:

$$U^{\text{sym}} = \frac{C_{\text{sym}}}{2} [(\gamma - 1)u_i^\gamma \delta_i^2 \pm 2u_i^\gamma \delta_i] \quad (5)$$

$$u_i = \frac{\langle \rho \rangle_i}{\rho_0}, \delta_i = \frac{\langle \rho \rangle_i^n - \langle \rho \rangle_i^p}{\langle \rho \rangle_i}$$

where C_{sym} is the strength of symmetry energy at saturation density, γ is the symmetry energy stiffness coefficient, and the symbol “+” for neutrons, “-” for protons.

The MDI can be written as follows:

$$U^{\text{MDI}} = \delta \ln^2[\varepsilon(\frac{\rho}{\rho_0})^2 + 1](\frac{\rho}{\rho_0}) \quad (6)$$

where $\delta=1.57 \text{ MeV}$, $\varepsilon=500 \text{ c}^2/\text{GeV}^2$.

represent the equation of state are given in Table 1. In the table, S(M) represents the soft EOS (with the MDI); H(M) represents the hard EOS (with the MDI).

2.2 Formulism and Method

The dipole moment of GDR in coordinator space and momentum space can be defined as follows^[26,27]:

$$DR_{\text{GDR}}(t) = \frac{NZ}{A} [R_Z(t) - R_N(t)] \quad (7)$$

$$DK_{\text{GDR}}(t) = \frac{NZ}{A\hbar} \left[\frac{P_Z(t)}{Z} - \frac{P_N(t)}{N} \right] \quad (8)$$

Here, $R_Z(t)$ and $R_N(t)$ represent the Center of Mass (CM) of protons and neutrons in coordinator space, respectively; $P_Z(t)$ and $P_N(t)$ represent the CM of protons and neutrons in momentum space, respectively.

By the Fourier transformation of the second derivative of $DR_{\text{GDR}}(t)$ in respect of time:

$$DR''(\omega) = \int_{t_0}^{t_{\text{max}}} DR''(t) e^{i\omega t} dt \quad (9)$$

one can get the photon emission probability for energy $E_\gamma = \hbar\omega$ as follows:

$$\frac{dP}{dE_\gamma} = \frac{2e^2}{3\pi\hbar c^3 E_\gamma} |DR''(\omega)| \quad (10)$$

Similarly, the dipole moment of PDR in coordinator space and momentum space can be defined as follows:

$$DR_{\text{PDR}}(t) = \frac{N_v Z}{A} [R_C(t) - R_{N_v}(t)] \quad (11)$$

$$DK_{\text{PDR}}(t) = \frac{N_v Z}{A\hbar} \left[\frac{P_C(t)}{2Z} - \frac{P_{N_v}(t)}{N_v} \right] \quad (12)$$

Here, $R_C(t)$ and $R_{N_v}(t)$ represent the CM of the isospin-symmetric core and the valence neutrons in coordinator space, respectively; $P_C(t)$ and $P_{N_v}(t)$

represent the CM of the isospin-symmetric core and the valence neutrons in momentum space, respectively. Then the photon emission probability of PDR can be also obtained.

In PDR calculation, a key point is how to choose the valence neutrons in the simulation. In our calculations, we choose the neutrons with the farthest distance from the CM of all nucleons as the valence neutrons in the initial state, and extract their oscillation character in the following dynamical process.

The fraction of Energy-Weighted Sum Rule (EWSR) contained in the PDR relative to that located in the GDR region can be written as follows:

$$\text{EWSR \%} = \frac{\text{PDR}_{m_1}}{\text{GDR}_{m_1} + \text{PDR}_{m_1}} \times 100\% \quad (13)$$

where the PDR_{m_1} is EWSR of PDR and GDR_{m_1} is GDR, i.e.:

$$\text{GDR}_{m_1} = \sum_{E_1}^{E_2} \left(\frac{dP}{dE_\gamma} \right)_{\text{GDR}} \Delta E \times E \quad (14)$$

$$\text{PDR}_{m_1} = \sum_{E_1'}^{E_2'} \left(\frac{dP}{dE_\gamma} \right)_{\text{PDR}} \Delta E \times E \quad (15)$$

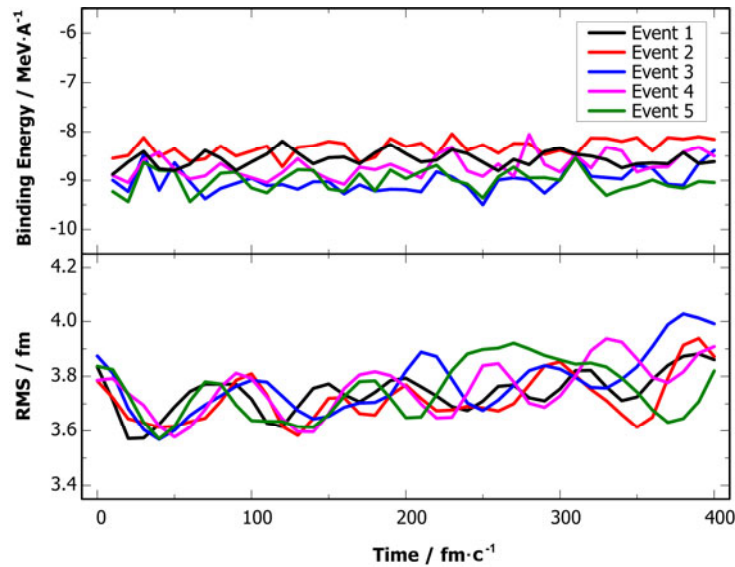


Fig.1 Time evolutions of the root mean square radii and of the binding energy for some samples of stable nuclei of ^{68}Ni . Soft EOS w/ MDI.

3 Results and discussions

In the present low energy transport model simulations, the stability check for the nucleus is always important. To this end, we have to pick up the stable nucleus in the initialization. For an example, the time evolution of the root mean square radii and the binding energy of some stable nuclei are shown in Fig.1. Clearly, both the root mean square radii and the binding energy are stable with the time evolution before $400 \text{ fm}\cdot\text{c}^{-1}$.

Using the above stable nuclei to do Coulomb excitation simulation with the IQMD, one can get the spectrum of photon emission. Here ^{197}Au is chosen as the target, and only the GDR or PDR spectrum of the collective motion of nucleons inside projectile (Ni isotopes) is calculated. By a Gaussian fitting to the

spectra, the peak energy and strength can be extracted. Then their sensitivities to impact parameter, incident energy and the strength of symmetry energy can be also investigated. The sensitivities of these parameters to impact parameter have been given in Fig.2. It shows that the peak energies and strengths of both GDR and PDR do not change much with the impact parameter increasing. Considering that the impact parameter changes from 16 fm to 26 fm, which makes the Coulomb excitation just change a little, this result is reasonable.

Figure 3 shows the incident energy dependence of GDR and PDR parameters for ^{68}Ni .

When the incident energy increases, both the peak energies and strengths of GDR and PDR decrease. With the increasing of incident energy, the projectile

goes through the Coulomb field of target more quickly so that the Coulomb excitation becomes smaller, and then the projectile gets less excited.

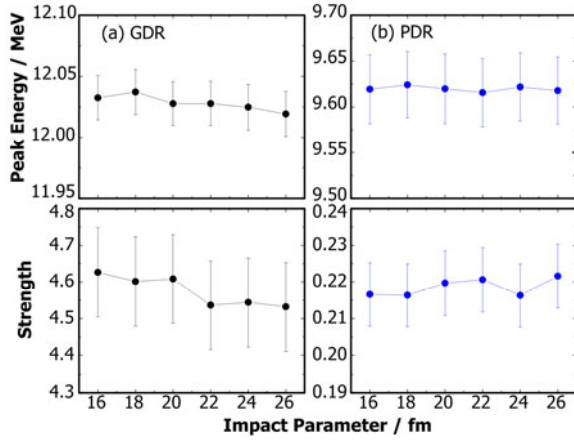


Fig.2 Impact parameter dependence of GDR and PDR parameters for ^{68}Ni . In calculations, we use $E_{\text{in}}=600$ MeV/nucleon, $C_{\text{sym}}=32$ MeV, $\gamma=1$, and the Soft EOS w/o MDI.

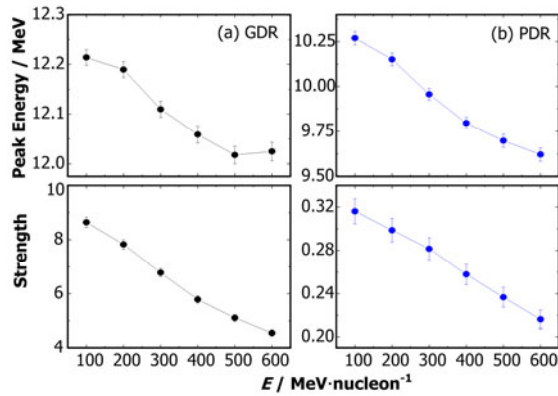


Fig.3 Incident energy dependence of GDR and PDR parameters for ^{68}Ni . In calculations, we use $b=24$ fm, $\gamma=1$, $C_{\text{sym}}=32$ MeV, and the Soft EOS w/o MDI.

As well known, symmetry energy is very important in nuclear physics and astrophysics. In some previous studies, PDR has been shown as a useful probe to investigate symmetry energy. Here we also investigate the relationship between PDR and symmetry energy. In our IQMD model, the symmetry energy can be written as:

$$E_{\text{sym}} = 12.5 \left(\frac{\rho}{\rho_0} \right)^{2/3} + \frac{C_{\text{sym}}}{2} \left(\frac{\rho}{\rho_0} \right)^{\gamma} \quad (16)$$

where the first term is the kinetic energy term and the second term is the potential term, γ is the symmetry energy stiffness coefficient. We study the relationship between the two parameters, i.e., C_{sym} and γ in the symmetry energy formula, and the parameters of PDR.

Fig.4 shows the strength of symmetry energy C_{sym} dependence of GDR and PDR parameters for ^{68}Ni . With the C_{sym} increasing, the peak energy of GDR increases, while that of PDR decreases and both strengths of GDR and PDR decrease. The γ dependence of GDR and PDR parameters for ^{68}Ni is shown in Fig.5. With γ increasing, the peak energy of GDR decreases, while that of PDR increases and both strengths of GDR and PDR increase.

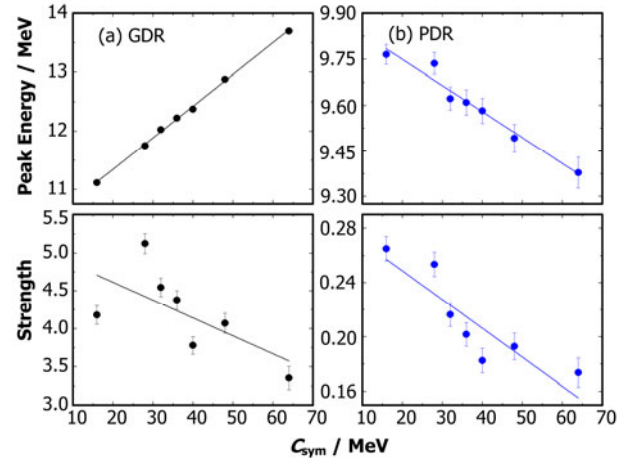


Fig.4 C_{sym} dependence of GDR and PDR parameters for ^{68}Ni . In calculations, we use $E_{\text{in}}=600$ MeV/nucleon, $b=24$ fm, $\gamma=1$, and the Soft EOS w/o MDI.

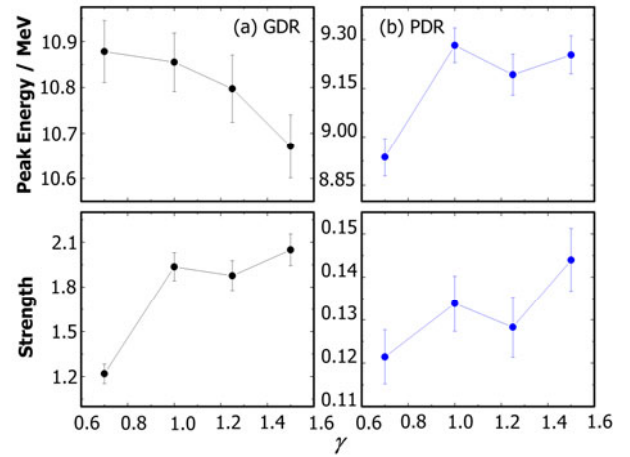


Fig.5 γ dependence of GDR and PDR parameters for ^{68}Ni . In calculations, we use $E_{\text{in}}=600$ MeV/nucleon, $b=24$ fm, $C_{\text{sym}}=35.2$ MeV, and Soft EOS w/o MDI.

Figures 4 and 5 show different behaviors of the peak energy of GDR and PDR: i.e. the peak energy of GDR increases with the C_{sym} increasing, and decreases with the γ increasing, For PDR, the peak energy decreases with the C_{sym} increasing, and increases with the γ increasing. To understand these questions, Fig.6

shows the symmetry energy versus C_{sym} and γ . Since we use Coulomb excitation method in our calculation, the density of nucleon in projectile is mainly in sub-saturation area. By the line for guiding eyes in Fig.6, one can see that the symmetry energy increases with C_{sym} increasing when γ is always fixed to be 1 (Fig.6a), and decreases with the γ increasing in sub-saturation area (Fig.6b). So the peak energy of GDR has a positive correlation with symmetry energy, but for PDR an anti-correlation with symmetry energy is shown.

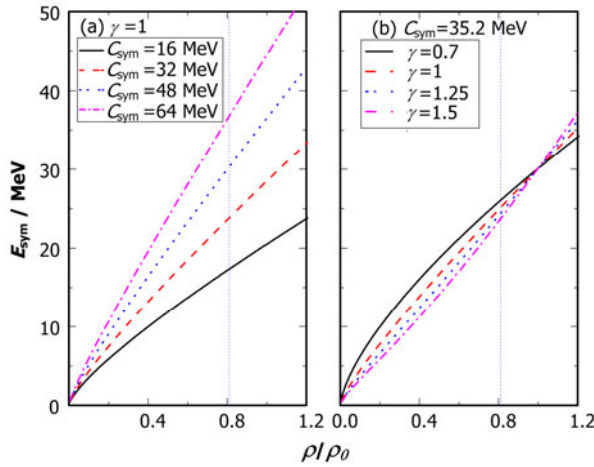


Fig.6 E_{sym} vs. ρ/ρ_0 with various C_{sym} or γ . (a) γ is fixed to be 1; and (b) C_{sym} is fixed to be 35.2 MeV.

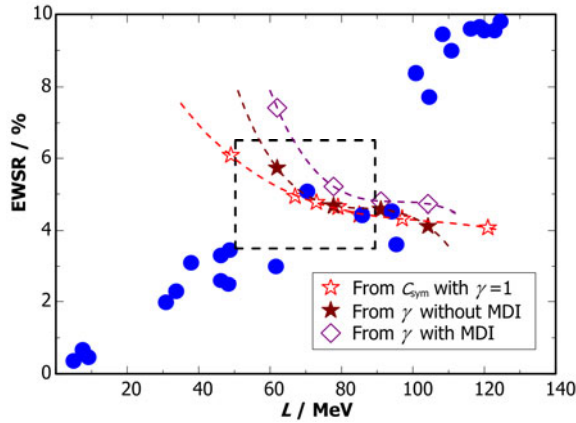


Fig.7 EWSR vs. the derivative of the symmetry energy at saturation (L).

In previous studies, a good correlation between L (the derivative of the symmetry energy at saturation) and the fraction of energy-weighted sum rule (in percentage) exhausted by the PDR in ^{68}Ni has been built-up^[28]. Different mean-field calculation results^[28] for ^{68}Ni are displayed in the Fig.7, where the solid circles

represent those results. From the symmetry energy Eq.(16), one can get the L as follows:

$$L = 25 + \frac{3}{2}C_{\text{sym}} \cdot \gamma \quad (17)$$

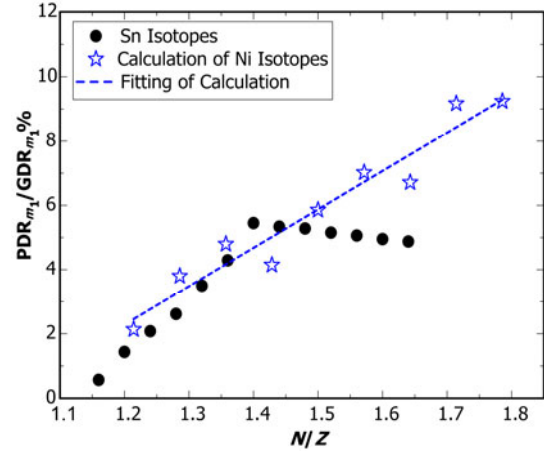


Fig.8 EWSR ($\text{PDR}_{m_1} / \text{GDR}_{m_1} \%$) vs. N/Z . In calculations, we use $E_{\text{in}}=100$ MeV/nucleon, $b=24$ fm, $C_{\text{sym}}=32$ MeV, $\gamma=1$, and the Soft EOS w/o MDI.

From the above equation, L increases linearly with either C_{sym} or γ when another is fixed. Our calculation results are shown in open stars, solid stars and open diamonds, respectively, for the L deduced from the different C_{sym} for $\gamma=1$ (soft EOS w/o MDI), from the different γ where $C_{\text{sym}}=35.2$ MeV (soft EOS w/o MDI), and from the different γ where $C_{\text{sym}}=35.2$ MeV (soft EOS w/ MDI). It is found that EOS with MDI gets higher fraction of EWSR compared with that without MDI. This may be due to the effective mass reduced by MDI. The curves are their polynomial fits, from which one can estimate the range of L and C_{sym} for our IQMD model. The box in the figure shows the constraints from experiments and other calculations^[8]. Within this box C_{sym} and γ in IQMD model can be limited from the crossing-points of of fitting curves. In the case of $\gamma=1$ for the Soft EOS w/o MDI, one can get $C_{\text{sym}} \in [16.9, 42.9]$ MeV if we take $L \in [50.3, 89.4]$ as Ref.[8]. In the case of $C_{\text{sym}}=35.2$ MeV for the Soft EOS w/o MDI, we obtain $\gamma \in [0.61-1.22]$ and $L \in [57-89.4]$ MeV. In the case $C_{\text{sym}}=35.2$ MeV for the Soft EOS w/ MDI, $\gamma \in [0.78-1.22]$ and $L \in [66-89.4]$ MeV. Based on the above results, the symmetry energy with too soft or too stiff density dependence should be excluded.

Finally, we plot the fraction of EWSR ($\text{PDR}_{m_1} / \text{GDR}_{m_1} \%$) versus N/Z for our results together with Piekarewicz's^[17] in Fig.8. With the ratio of neutrons and protons increasing, our calculation results of Ni isotopes show a linear increasing; but for Piekarewicz's results of Sn isotopes within the framework of the relativistic random phase approximation, it shows a linear increasing firstly, and then a slightly linear decreasing.

4 Conclusion

In this paper, we studied PDR and GDR of Ni isotopes by the Coulomb excitation in the framework of IQMD model. By the Gaussian fitting to the photon spectra, we obtain parameters of GDR and PDR, such as the peak energy and strength. The sensitivities of these parameters to impact parameter, incident energy, and the symmetry energy are studied. The results show that the peak energies of GDR and PDR are correlated with symmetry energy and while EWSR% is anti-correlated with the derivative of the symmetry energy at saturation. Combining with the data and other calculation, we constrain the γ coefficient and L parameter for the IQMD with the different symmetry energy parameters, i.e. for the soft EOS w/o MDI, the γ is in 0.61–1.22 region and L is in 57–89.4 MeV, and while for soft EOS with MDI, γ is in 0.78–1.22 region and L is in 66–89.4 MeV. In the other word, too stiff or too soft symmetry energy form is excluded from the present calculations. At the last, the N/Z dependence of PDR and GDR parameters of Ni isotopes was studied. It shows that the fraction of EWSR ($\text{PDR}_{m_1} / \text{GDR}_{m_1} \%$) increases linearly with the N/Z .

References

- 1 Simenel C, Chomaz P, France de G. *Phys Rev Lett*, 2001, **86**: 2971–2974.
- 2 Baran V, Brink M D, Colonna M, *et al.* *Phys Rev Lett*, 2001, **87**: 182501.
- 3 Krewald S and Speth J. *Int J Mod Phys E*, 2009, **18**: 1425–1451.
- 4 Paar N, Vretenar D, Khan E, *et al.* *Rep Prog Phys*, 2007, **70**: 691–793.
- 5 Leistenschneider A, Aumann T, Boretzky K, *et al.* *Phys Rev Lett*, 2001, **86**: 5442–5445.
- 6 Hartmann T, Enders J, Mohr P, *et al.* *Phys Rev Lett*, 2000, **85**: 274–277.
- 7 Hartmann T, Babilon M, Kamerdzhev S, *et al.*, *Phys Rev Lett*, 2004, **93**: 192501.
- 8 Wieland O, Bracco A, Camera F, *et al.* *Phys Rev Lett*, 2009, **102**: 092502.
- 9 Adrich P, Klimkiewicz A, Fallot M, *et al.* *Phys Rev Lett*, 2005, **95**: 132501.
- 10 Fultz S C, Berman B L, Caldwell J T, *et al.*, *Phys Rev*, 1969, **186**: 1255–1270.
- 11 Ryezayeva N, Hartmann T, Kalmykov Y, *et al.* *Phys Rev Lett*, 2002, **89**: 272502.
- 12 Liang J, Cao L G, Ma Z Y. *Phys Rev C*, 2007, **75**: 054320.
- 13 Tselyaev V, Speth J, Grummer F, *et al.* *Phys Rev C*, 2007, **75**: 014315.
- 14 Paar N, Vretenar D, and Ring P, *Phys Rev Lett*, 2005, **94**: 182501.
- 15 Tao C, Ma Y G, Zhang G Q, *et al.* *Phys Rev C*, 2013, **87**: 014621.
- 16 Barbieri C, Caurier E, Langanke K, *et al.* *Phys Rev C*, 2008, **77**: 024304.
- 17 Piekarewicz J, *Phys Rev C*, 2006, **73**: 044325.
- 18 Liu G M, Fu D, Ma Y G, *et al.* *Chin J Nucl Phys*, 1993, **15**: 234.
- 19 Baran V, Frecus B, Colonna M, *et al.* *Phys Rev C*, 2012, **85**: 051601(R).
- 20 Aichelin J. *Phys Rep*, 1991, **202**: 233.
- 21 Hartnack C, Puri R K, Aichelin J, *et al.* *Eur Phys J A*, 1998, **1**: 151–169.
- 22 Hartnack C, Li Z X, Neise L, *et al.* *Nucl Phys A*, 1989, **495**: 303–319.
- 23 Ma Y G, Wei Y B, Shen W Q, *et al.* *Phys Rev C*, 2006, **73**: 014604.
- 24 Zhang G Q, Cao X G, Fu Y, *et al.* *Nucl Sci Tech*, 2012, **23**: 61–64.
- 25 Li S X, Fang D Q, Ma Y G, *et al.* *Nucl Sci Tech*, 2011, **22**: 235–239.
- 26 Baran V, Cabibbo M, Colonna M, *et al.* *Nucl Phys A*, 2001, **679**: 373–392.
- 27 Wu H L, Tian W D, Ma Y G, *et al.* *Phys Rev C*, 2010, **81**: 047602.
- 28 Wieland O and Bracco A, *Prog Part Nucl Phys*, 2011, **66**: 374–378.